First publ. in: Journal of Histochemistry and Cytochemistry 48 (2000), 9, pp. 1269-1281

Quantitative Immunogold Localization of Protein Phosphatase 2B (Calcineurin) in *Paramecium* Cells

M. Momayezi, R. Kissmehl, and H. Plattner

Faculty of Biology, University of Konstanz, Konstanz, Germany

SUMMARY For immunogold EM labeling analysis, we fixed *Paramecium* cells in 4% formaldehyde and 0.125% glutaraldehyde, followed by low-temperature embedding in unicryl and UV polymerization. We first quantified some obvious but thus far neglected side effects of section staining on immunogold labeling, using mono- or polyclonal antibodies (Abs) against defined secretory and cell surface components, followed by $F(ab)_2$– or protein A–gold conjugates. Use of alkaline lead staining resulted in considerable rearrangement and loss of label unless sections were postfixed by glutaraldehyde after gold labeling. This artifact is specific for section staining with lead. It can be avoided by staining sections with aqueous uranyl acetate only to achieve high-resolution immunogold localization of a protein phosphatase on unicryl sections. In general, phosphatases are assumed to be closely, although loosely, associated with their targets. Because the occurrence of protein phosphatase 2B (calcineurin) in *Paramecium* has been previously established by biochemical and immunological work, as well as by molecular biology, we have used Abs against mammalian CaN or its subunits, CaN-A and CaN-B, for antigen mapping in these cells by quantitative immunogold labeling analysis. Using ABs against whole CaN, four structures are selectively labeled (with slightly decreasing intensity), i.e., infraciliary lattice (centrin-containing contractile cortical filament network), parasomal sacs (coated pits), and outlines of alveolar sacs (subplasmalemmal calcium stores, tightly attached to the cell membrane), as well as rims of chromatin-containing nuclear domains. In other subcellular regions, gold granules reached densities three to four times above background outside the cell but there was no selective enrichment, e.g., in cilia, ciliary basal bodies, cytosol, mitochondria, trichocysts (dense-core secretory organelles), and non-chromatin nuclear domains. Their labeling density was 4- to 8.5-fold (average 6.5-fold) less than that on selectively labeled structures. Labeling tendency was about the same with Abs against either subunit. Our findings may facilitate the examination of molecular targets contained in the selectively labeled structures.

KEY WORDS
calcineurin
ciliates
immunolocalization
Paramecium
phosphatase 2B
protozoa

A variety of cellular processes are regulated by protein kinases and phosphatases (Vincent and Crowder 1995). As a rule, after stimulation kinases frequently undergo relocalization, whereas phosphatases remain co-localized to their targets, to allow a sufficiently fast response despite a relatively slow reaction rate (Inagaki et al. 1994). Among the large number of Ser/Thr-phosphatases (Shenolikar 1994; Barford 1996; Cohen 1997), phosphatase 2B (PP2B, calcineurin, CaN) is activated by a Ca^{2+}/calmodulin (CaM) complex (Guerini and Klee 1991; Guerini 1997). CaN is made up of two subunits (Klee et al. 1998; Perrino and Soderling 1998). The catalytic subunit CaN-A, of 59-65 kD, possesses a catalytic domain, a CaN-B- and a CaM-binding domain, and an autoinhibitory domain, whereas CaN-B is 16–21 kD, binds Ca^{2+}, and is myristoylated at the N-terminus (Aitken et al. 1984; Boutin 1997). Binding of CaN to biomembranes and to some cytoskeletal elements is favored by Ca^{2+}/CaM-dependent association of the subunits (Huang et al. 1989; Klee et al. 1998).

CaN is widely distributed throughout eukaryotic

Correspondence to: H. Plattner, Faculty of Biology, University of Konstanz, 78434 Konstanz, Germany.

Received for publication December 2, 1999; accepted April 4, 2000 (9A5150).

cells, from the ciliated protozoan *Paramecium* (Momayezi et al. 1987; Hinrichsen et al. 1995; Kissmehl et al. 1997), the slime mold, *Dictyostelium* (Dammann et al. 1996), yeast (Cyert and Thorner 1992; Hirata et al. 1995), to mammals (Yakel 1997). It is involved in transcription activation (Hirata et al. 1995; Shibasaki et al. 1996; Chin et al. 1998; Lee et al. 1999), regulation of internal Ca^{2+} release channels (Valdivia 1998), modulation of some plasmalemmal ion channels (Fomina and Levitan 1997; Lukyanetz 1997; Schuhmann et al. 1997), and regulation of endocytosis via coated pits (Liu et al. 1994; Robinson et al. 1994; Marks and McMahon 1998). In particular, CaN may be involved in the regulation of exocytosis in widely different systems, from protozoa (Momayezi et al. 1987), pancreatic acinar cells (Groblewski et al. 1994), gastric chief cells (Raufman et al. 1997), mast cells (Hultsch et al. 1998), and some other non-neuronal cells (Groblewski et al. 1998) to neuronal systems (Nichols et al. 1994; Hens et al. 1998). There may exist many potential targets to which CaN may be localized. Even in nerve terminals where there are a multitude of phosphorylated proteins (Turner et al. 1999), any differential effects of CaN or of some other phosphatases remain to be elucidated.

In the ciliated protozoan *Paramecium tetraurelia*, immunological evidence first suggested the occurrence of CaN and a role in exocytosis regulation (Momayezi et al. 1987), but the cloning of the gene (Hinrichsen et al. 1995) and enzymatic as well as pharmacological characterization (Kissmehl et al. 1997) occurred much later. In these studies we recognized a 63- and a 17-kD subunit on Western blots using antibodies (Abs) that we prepared against complete CaN from bovine brain. These Abs have now been used for postembedding immunogold EM localization. We used non-permeabilized cells embedded in unicryl-type methacrylate resin in conjunction with low-temperature UV polymerization.

We applied low-temperature embedding to account for the fact that, in general, ~50% of CaN may be cytosolic, the other 50% being membrane bound (Yakel 1997). Sites of considerable enrichment of antigen can be identified most easily by the quantitative analysis we perform. To achieve this, it is essential to avoid any serious redistribution. Therefore, we add, as a technical note, our observation on section staining by alkaline lead citrate which, although frequently used, may blur originally clear-cut immunogold labeling. Sufficiently long staining with aqueous uranyl acetate is an easy alternative because this maintains high resolution and sensitivity by avoiding displacement and loss of gold granules.

This is the first ultrastructural immuno-EM (electron microscopic) localization of CaN. Among the intensely labeled structures in *Paramecium*, there are some targets to be expected from biochemical analyses but also some additional unexpected ones, thus providing important suggestions for future work. In detail, we find intensely labeled "infraciliary lattice" (cortical centrin-containing contractile filament system), outlines of "alveolar sacs" [suplasmalemmal calcium stores (Stelly et al. 1991; Länge et al. 1995)], docking sites of "trichocysts" (dense-core secretory organelles), "parasomal sacs" (coated pits), and chromatin-enriched nuclear domains. We also tried, although only qualitatively, to elaborate differential labeling with Abs against subunits A and B, all with the same pattern. Remarkably, the same methodology applied to localize some other protein phosphatases in *Paramecium*, PP1 (Momayezi et al. 1996) and PP2C (Grothe et al. 1998), gave quite different labeling patterns.

Materials and Methods

Cell Cultures

Paramecium tetraurelia wild-type cells (strain 7S) were cultivated as described (Plattner et al. 1997b).

Fixation and Embedding

Cells were fixed for 30 min at 4C in 4% formaldehyde plus 0.125% glutaraldehyde in PBS, pH 7.2, washed three times for 10 min each in PBS containing 50 mM glycine, and dehydrated in increasing ethanol concentrations (30, 50, 70, 90, and 2 times 100%, 5 min each). This was followed by impregnation with unicryl resin (British BioCell; London, UK) at 0C, with two changes at 2-hr intervals and then overnight, followed by UV polymerization at −25C for 24 hr.

Antibody Labeling

Ultrathin sections collected on formvar-coated nickel grids were pretreated twice for 10 min with 20 μl of PBS + glycine (50 mM) and then immersed in PBS supplemented with 0.5% bovine serum albumin (BSA) and 0.5% goat serum for 10 min at room temperature (RT), to eliminate nonspecific gold adsorption. Then the grids were incubated with primary Abs diluted in PBS supplemented with 0.2% BSA-c (BioTrend; Köln, Germany) pH 7.4, for 1 hr at RT (or for 24 hr at 4C). Ab dilutions were 1:30. Note that BSA-c is an acetylated form which, due to increased net charge, reduces nonspecific adsorption of gold conjugates.

The primary Abs used were anti-CaN (subunit A+B) Abs (designated R299) as specified previously (Kissmehl et al. 1997; Hens et al. 1998) and Abs against subunit A (Stressgen; Victoria, BC, Canada) or B (Affinity Bioreagents; Golden, CO). All these Abs were polyclonal Abs from rabbit directed against antigens isolated from bovine brain.

Samples were washed in PBS/BSA-c, three times for 10 min each, and treated for 1 hr with gold conjugates. We used either goat anti-rabbit (GαR) IgGs, $F(ab)_2$ fragments derived from these GαR IgGs, or protein A (pA), coupled to 5- or 10-nm gold (Au_5, Au_{10}) as indicated. Gold conjugates

of IgGs and of pA were from BioTrend and from the University of Utrecht (Department of Cell Biology, School of Medicine, Utrecht, The Netherlands), respectively. Dilution was 1:20 for Ab–gold conjugates and 1:40 for pA–gold conjugates.

The specificity of immunogold labeling was verified by a significant reduction in the number of gold particles on sections incubated with Abs preadsorbed with the original antigen, i.e., Abs against CaN from bovine brain (50 μg/ml of diluted Ab solution).

After labeling, sections were rinsed with distilled water, fixed for 5 min with 2% glutaraldehyde, and routinely stained for 5 min with 2% aqueous uranyl acetate only (un-

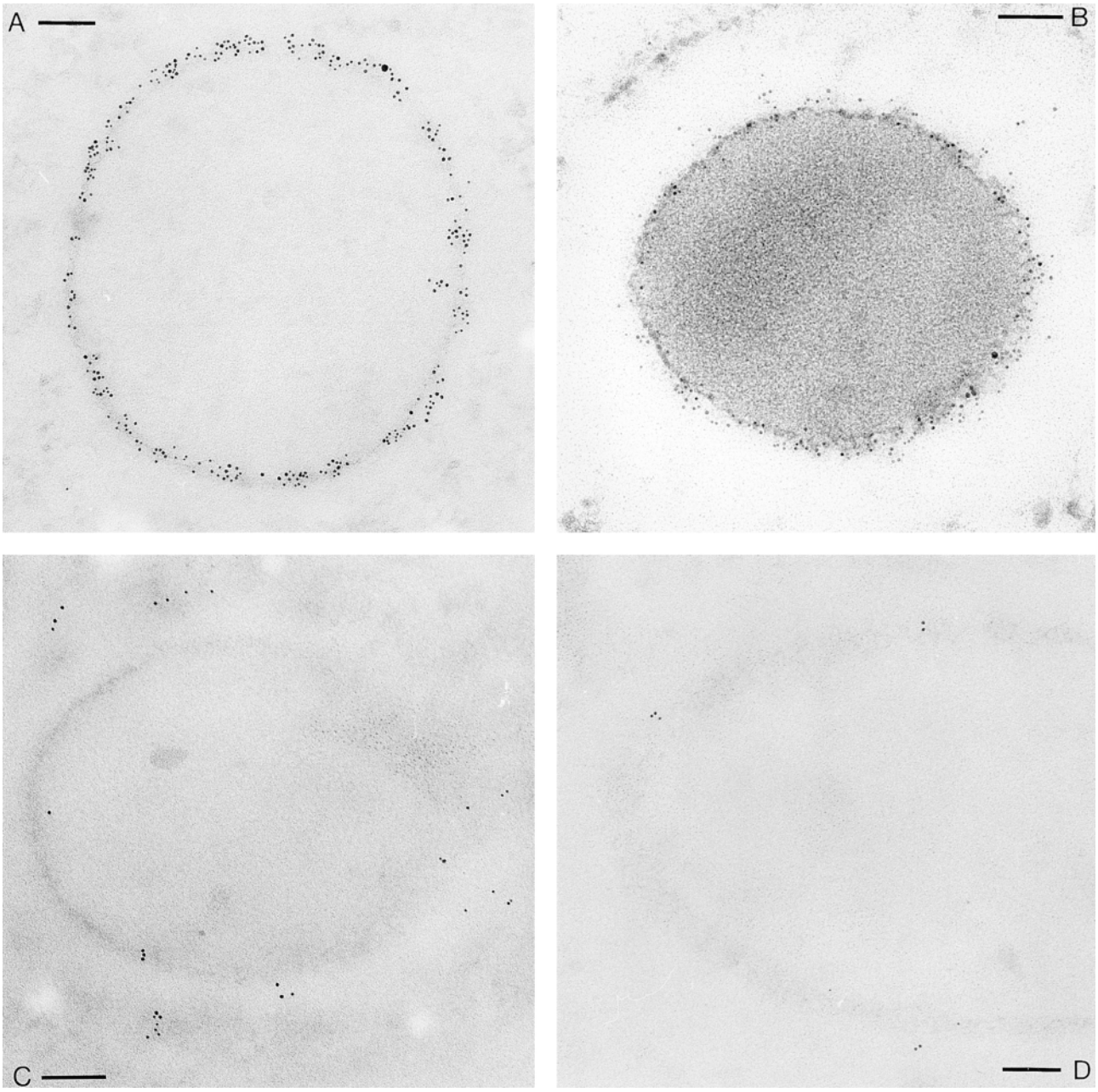

Figure 1 Effect of section staining on labeling density, as exemplified with Abs against the "mesh-like sheath" component, localized between the dense core of secretory materials and the trichocyst membrane, using monoclonal primary Abs followed by GαM–Au_5. (**A**) Section not fixed after labeling, staining with uranyl. (**B**) Section fixed after labeling, then stained with uranyl and lead. (**C**) Section stained with lead, without fixation between labeling and staining. (**D**) Section not fixed after labeling, stained with uranyl and lead. Labeling is most intense and that localization most precise with uranyl staining only (**A**) or, if sections are fixed before staining, also with uranyl/lead sequential double staining (**B**), whereas lead staining at pH 12.0 (**D**) or mere exposure to pH 12.0 (not shown) without previous fixation causes redistribution and considerable loss of label. Bars = 0.1 μm.

buffered, pH 4.5). In experiments on the effects of section staining, these parameters were varied as follows.

Effect of Section Staining on Ab Labeling

We analyzed the effect of alkaline lead citrate, frequently used as a standard stain, on immunogold labeling (Figure 1). We used monoclonal Abs (MAbs) against a well-defined secretory component, the "mesh-like sheath" (which in *Paramecium* links the contents of a trichocyst with its membrane) as previously specified (Momayezi et al. 1993). We also tested polyclonal Abs from rabbit directed against *Paramecium* cell surface (glycocalyx) components as specified by Flötenmeyer et al. (1999). We then applied the same immunogold conjugates as indicated above.

Then the gold-labeled sections were processed either with or without 5-min fixation with 2% glutaraldehyde. Sections were stained in different ways, either with 2% aqueous (acidic) uranyl acetate as above or with standard alkaline lead citrate (Reynolds 1963; Venable and Coggeshall 1965), each for 5 min, or with both stains in sequence. In addition, we explored the effects of pH of either stain, i.e., 4.5 and 12.0, respectively, using appropriate buffers of low ionic strength. [Ionic strength per se had no effect, as we found by application of Tris-buffered saline (TBS), 200 mM.] Quantitative evaluation was done on randomly taken photographs as follows.

Evaluation of Labeling Density

Gold grains were counted on distinct structures of randomly taken samples and referred to area size of the respective structure analyzed (Kissmehl et al. 1998). Area size was determined by the "hit point method" as previously described (Plattner and Zingsheim 1983).

Results

Effects of Section Staining with Lead

We show some extreme situations occurring after gold labeling followed by application of different section staining procedures. Two different labelings were analyzed: (a) with MAbs against a defined secretory component contained in trichocysts, followed by $F(ab)_2$ goat anti-mouse IgG–Au_5 conjugates (Figures 1 and 2A), and (b) with rabbit Abs against glycocalyx components, followed by pA–Au_{10} (Figure 2B). Briefly, lead stain at pH 12.0, or just application of pH 12.0, caused dramatic redistribution and loss of gold label. This can be impeded by fixation of sections after immunogold labeling. This step is not required when uranyl only is applied. In this case, labeling density is approximately the same with or without section fixation.

Quantitative evaluation (Figure 2) revealed approximately the same effects with both labeling procedures analyzed, using either $F(ab)_2$– or pA–gold conjugates. Therefore, our findings may be of general interest. Essentially, we established the following details highlighted in Figure 1 and summarized in Figure 2. (a) Aqueous uranyl acetate (pH 4.5), a standard electron "stain" used to enhance structural contrast, does not impair immunogold labeling. This includes two aspects, sensitivity and structure–label correlation, i.e., the number of gold grains per area is large and grains are strictly asscociated with the respective structures ("mesh-like sheath" and glycocalyx components, respectively). Quantification substantiates that the situation does not improve when sections are fixed with glutaraldehyde before uranyl staining. The other extreme is staining with alkaline (pH 12.0) lead solution (Figure 1C) which, although frequently used to further enhance structural contrast even in immunocytochemical work, causes severe dislocation and even loss of

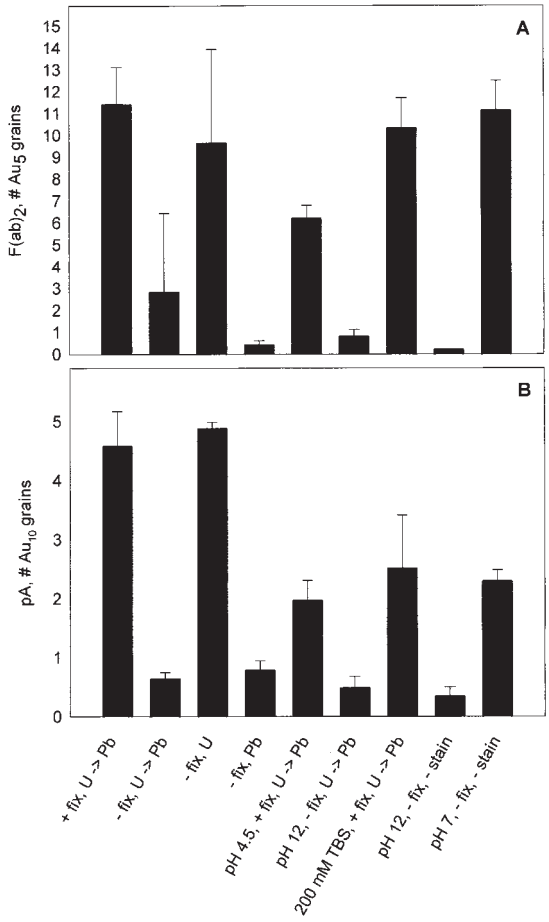

Figure 2 Quantitative evaluation of the different section staining protocols, as exemplified in Figure 1. Abs used in **A** were directed against the secretory component shown in Figure 1 (GαM–Au_5) and those used in **B** against glycocalyx components (pA–Au_{10}), as specified in "Materials and Methods." Note occurrence of the same tendencies with both sets of data, i.e., loss of labeling by application of lead stain or merely of pH 12.0 when sections were immunogold-labeled and stained without section fixation in between. Bars = SD; data collected from different areas, each in three cells per sample. For further evaluation and comments, see text.

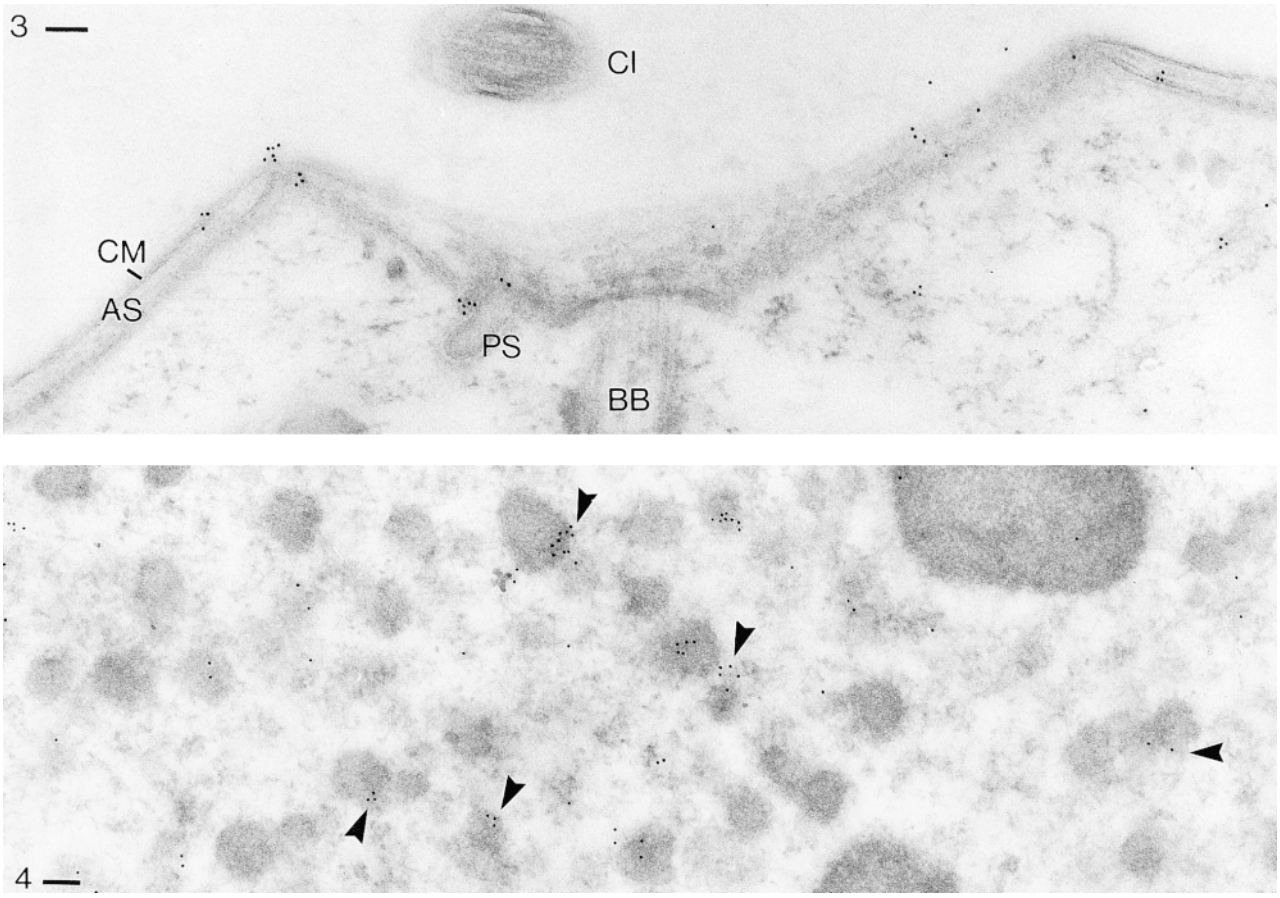

Figure 3 Anti-CaN Ab (R299), followed by GαR Ab-Au_{10}, labels the complex formed by cell membrane (CM) and alveolar sacs (AS), of which only the inner alveolar sac membranes can be recognized separately. Although a "parasomal sac" (PS) is labeled, a cilium (Cl) and a ciliary basal body (BB), as well as internal structures, are not specifically labeled. Bar = 0.1 μm.

Figure 4 Same procedure as in Figure 3, producing labeling of nuclear components, notably of the rims of heterochromatic areas (e.g., at arrowheads). Bar = 0.1 μm.

gold grains (Figures 2A and 2B). This artifact cannot be eliminated by uranyl application before lead staining (Figures 1D and 2A, B). Mimicing the high pH, essential for the lead stain to work (Reynolds 1963), causes the same artifact (Figure 2). Increasing ionic strength at neutral pH does not cause any significant loss of label.

In consequence, we recommend section staining with aqueous uranyl acetate only, section fixation after gold labeling not being mandatory. However, postfixation must be applied if structural contrast should be further increased by successive staining with uranyl and lead. In the analyses shown below, we applied only uranyl staining followed by fixation.

Localization of CaN Using Anti-CaN Abs (R299)

These Abs (designated R299) were prepared against whole bovine brain CaN and have been characterized on Western blots, not only with CaN subfractions obtained from *Paramecium* (Kissmehl et al. 1997) but also with some substrates from mammalian cells (Hens et al. 1998). To account for the notorious fluctuations in immunogold labeling intensity, these were evaluated quantitatively. Examples for immunolocalization are shown in Figures 3 to 6. Only much later (when our quantitative evaluations presented in Figure 9 were already finished) did Abs directed against subunits A and B from mammalian CaN become available. Results obtained with these new Abs are documented in Figures 10–15.

Figure 3 demonstrates the occurrence of label on the cell surface membrane complex. Because this is formed by the cell membrane and the closely apposed flat alveolar sacs, specific assignment of label to the cell membrane and to inner and outer regions of alveolar sacs, is not always possible. Some situations in Figure 3 and in some subsequent images suggest that

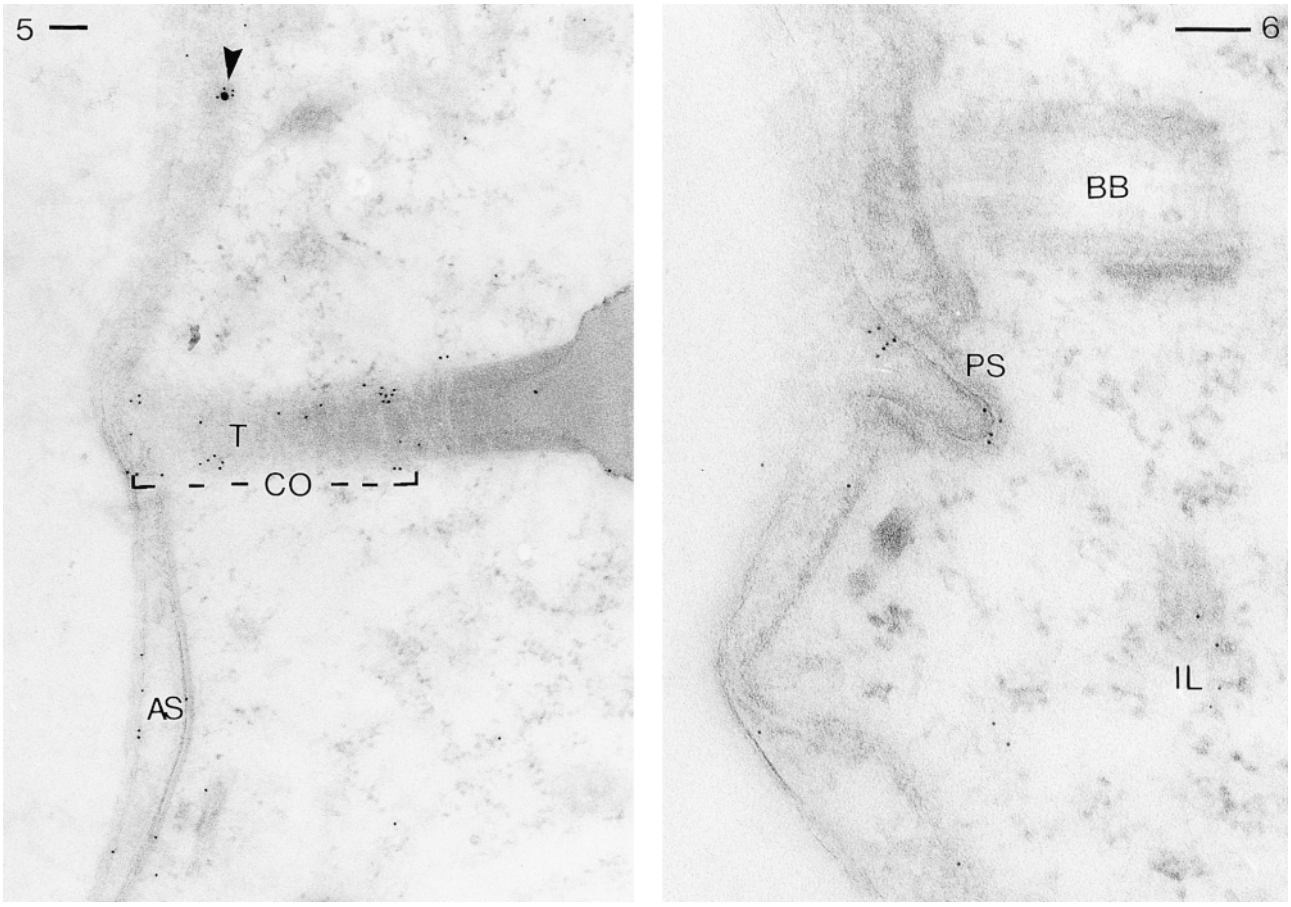

Figure 5 Trichocyst (T) docking site cut in an oblique angle. Ab application as in Figure 3 labels the uppermost region of a trichocyst surface ("collar" region, CO), where it emerges into the section surface, as well as the docking site proper. Some gold grains are also scattered over the surface complex as in Figure 3, including the inner membrane region of an alveolar sac (AS, arrowheads). Bar = 0.1 μm.

Figure 6 Same procedure as in Figure 3, but applying GαR–Au_5. Note intense labeling of a coated pit ("parasomal sac," PS) closely associated with a ciliary basal body (BB), moderate labeling of an "infraciliary lattice" (IL) component, and occurrence of only a few gold grains elsewhere in the cell cortex. Bar = 0.1 μm.

not only the inner side of alveolar sacs (or closely apposed materials) but also the much tighter complex formed by the outer part of alveolar sacs and the cell membrane is labeled. Figure 3 also shows significant labeling of a parasomal sac, with a few gold granules scattered in the cytosol.

Figure 4 is an example of significant labeling in the (macro-)nucleus. Label may be concentrated on regions with electron dense (hetero-)chromatin, or with their rims.

Because trichocyst docking sites are not frequently encountered, they are documented separately. In Figure 5, a docking site is cut tangentially. Therefore, much of its membrane-associated materials surrounding the upper two thirds of the narrow trichocyst tip are exposed. It is precisely this "collar" region (cf. Pouphile et al. 1986) that is intensely labeled, as is the uppermost region where a trichocyst is tied to alveolar sacs and the plasma membrane (docking site proper).

Figure 6 documents in more detail labeling of a parasomal sac or of its apical and basal regions. In this figure the sac can be easily identified by its association with a ciliary basal body, which is not labeled. Another structure not so commonly encountered is the infraciliary lattice, formed of filament bundles enriched in centrin. This is also regularly labeled.

Figures 7 and 8, showing again a cortical cell region, demonstrate the specificity of the type R299 Ab. The inner part of alveolar sacs (their "inner membrane") and the contractile "infraciliary lattice" are clearly labeled in Figure 7, in contrast to Figure 8. This difference is due to the use of Abs before (Figure 7) and after (Figure 8) preadsorption with the original antigen, before section labeling with GαR–Au_5.

In summary, after statistical evaluation of a great

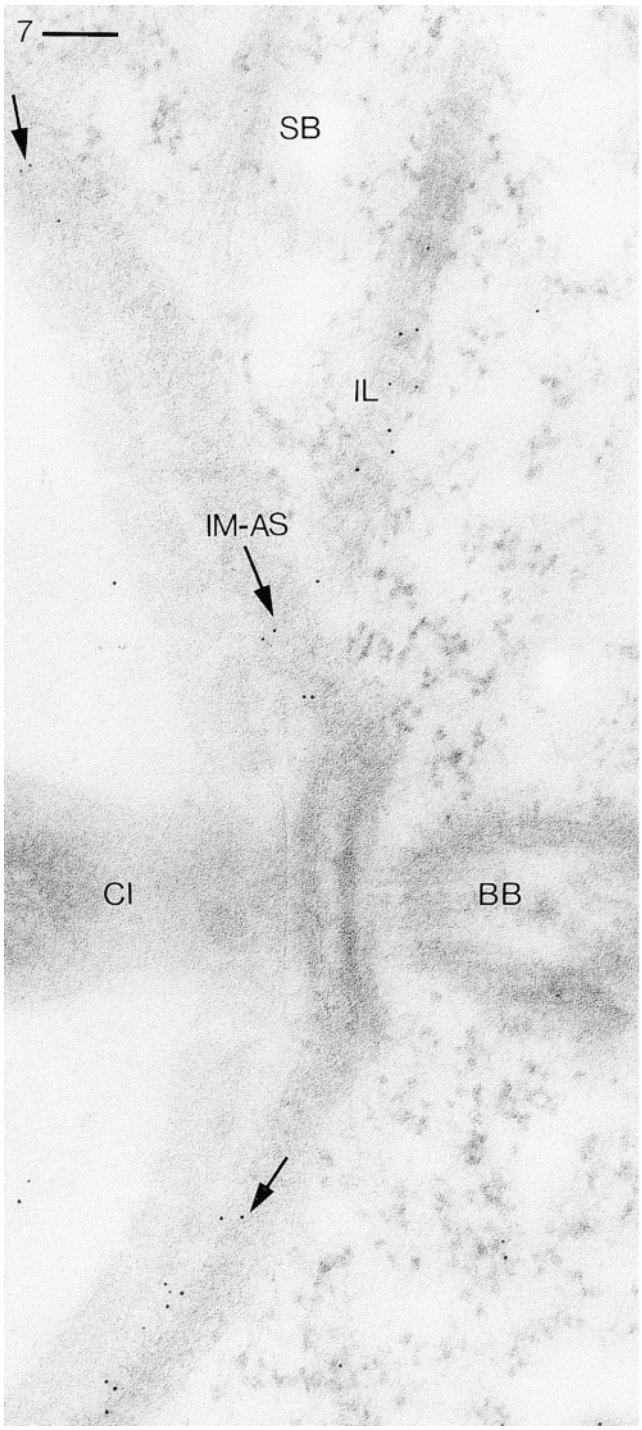

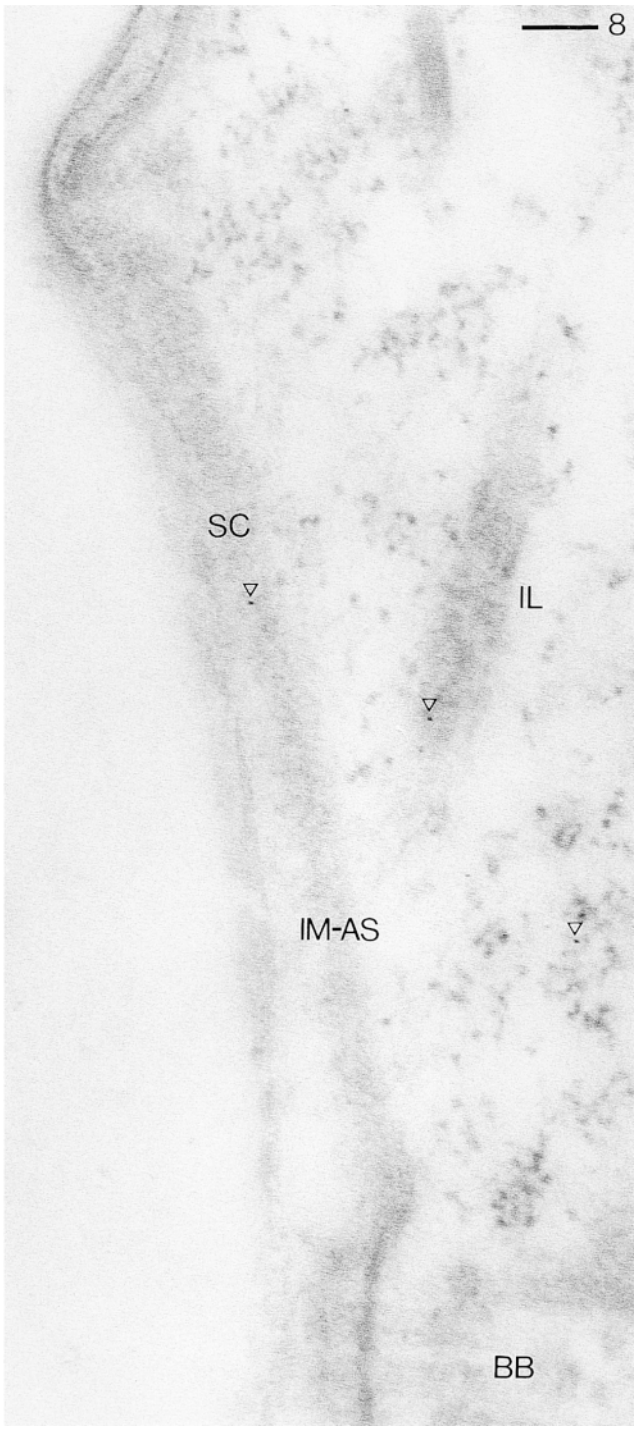

Figure 7 Same procedure as in Figure 3. Application of Ab type R299 followed by GαR–Au_5 labels the inner membrane region of alveolar sacs (IM-AS) in regions below arrows and that part of the "infraciliary lattice" (IL) where it evidently emerges onto the section plane (lower part). Note absence of any significant label from cytosol, from a "striated band" (SB, noncontractile cortical filament bundle), and from a cilium (CI) and its basal body (BB). Bar = 0.1 μm.

Figure 8 Same procedure as in Figure 3 (detail to be compared to Figure 7), but using R299 Abs after preadsorption with bovine brain CaN. This causes disappearance of most of the GαR–Au_5 label, except for a very few granules (arrowheads) on the inner membrane of alveolar sacs (IM-AS), on the "infraciliary lattice" (IL), and in the cytosol. BB, basal body; SC, surface membrane comples. Bar = 0.1 μm.

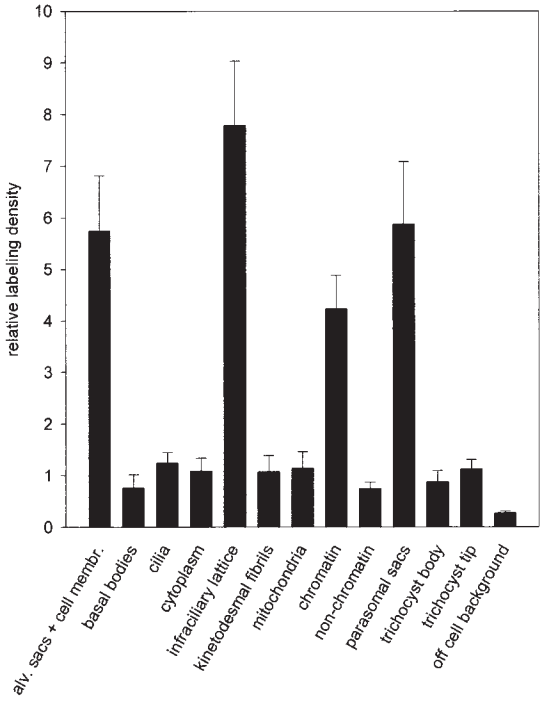

Figure 9 Quantitative evaluation of the structures selectively labeled under conditions presented in Figures 3 to 6 using Abs type R299 against whole CaN. Bars = SEM; sample size $n = 25$ for each bar.

number of samples to take into account the wide variability of labeling densities, the four regularly labeled structures in *Paramecium* are the cell surface complex (alveolar sacs + cell membrane), the infraciliary lattice, parasomal sacs, and chromatin borders (Figure 9).

Labeling with Abs Against Subunits of CaN

Examples of labeling with ABs against CaN-A are shown in Figures 10 and 11. On Western blots, Abs against the A- and the B-subunit strongly and selectively react with the respective subunits (data not shown). Although the labeling intensity achieved on ultrathin sections may be somewhat less than with Abs against both subunits (R299), the tendencies are all the same, as shown below.

In Figure 10, the surface membrane complex is cut tangentially and therefore displays rather intense labeling. Figure 10 also contains two parasomal sacs in oblique (bottom left) or cross-section (middle right). In both situations they are clearly labeled, as is some basal body-associated material. Figure 11 shows labeling of an emerging trichocyst docking site, although in this particular case much less cytosolic labeling and labeling of the surface membrane complex is present.

Similar situations are shown in Figures 12 and 13 for Abs against the B-subunit. Again, in Figure 12, the surface complex of cell membrane and alveolar sacs is labeled, as is a cross-cut parasomal sac. Figure 13 is a detail containing an emerging trichocyst whose docking site is again intensely labeled.

Figures 14 and 15 document for Abs against the A- and B-subunit, respectively, that in the macronucleus heterochromatic areas are preferentially stained, notably at their periphery. These data correspond to those with Ab type R299.

Discussion

Technical Note

CaN may only partially be present in a doublet, particularly when not associated with a membrane. Therefore, we tried to avoid loss or displacement of antigen, as occurs with too weak fixation (Bittermann et al. 1992), because we fixed cells with formaldehyde supplemented by a tolerable although low concentration of glutaraldehyde. However, we now observed another artifact that was without precedent.

We found that gold label is displaced and even removed from antigenic sites when a section is stained with alkaline lead citrate and that this is due to its obligatory pH of 12.0. We found this with gold conjugates of Abs and of pA applied to unicryl sections. Because unicryl is one of the methacrylate resins most widely used in immunogold labeling studies, the deleterious effect of section staining with alkaline lead solution that we detected may be of more general importance, although embedding media other than unicryl have not yet been analyzed in this regard. This deleterious effect was unexpected because the use of this stain, in addition to aqueous uranyl acetate, is quite common, as one can recognize in monographs on immunocytochemistry. If increased contrast is desired, uranyl staining may be prolonged or the EM set-up must to be selected accordingly. We do not know whether the Ab–Au complex, or the antigen, or the antigen–Ab complex is actually removed. Because after any application of pH 12.0 gold grains still may be present, but at a greater distance from the original localization of the antigen, the latter possibility also appears feasible.

Molecular Identity of CaN Substrates

Only a few substrates of CaN are well characterized, so that immunolocalization may yield new hints. Well-defined targets are the PP1 inhibitors DARPP-32 (Desdouits et al. 1995) and NFAT (Shenolikar 1994), which are phosphorylated at Thr and Ser sites, respectively, some microtubule-associated proteins (Quinlan and Halpain 1996), transcription factor ELK-1 (Sugimoto et al. 1997), the monomeric GTP-binding protein dynamin (Nichols et al. 1994), and only a few

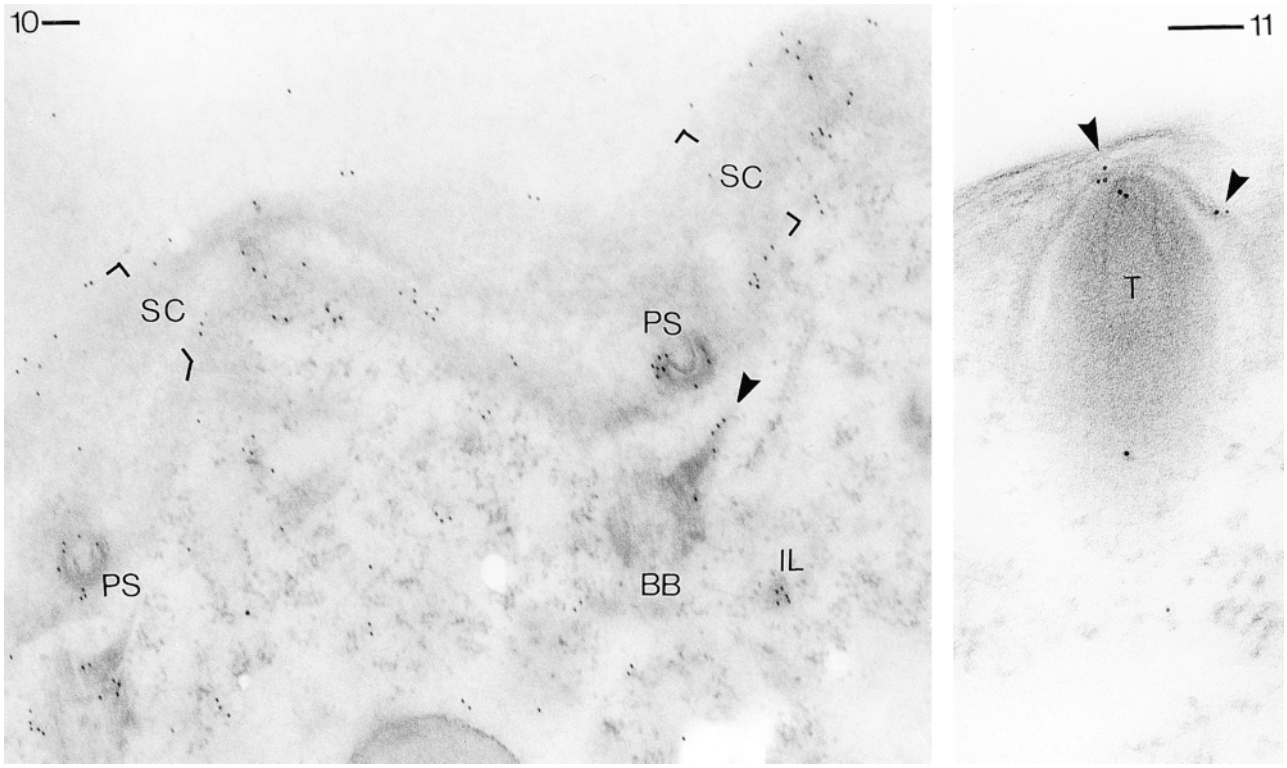

Figure 10 Labeling by Abs against CaN-A and GαM-Au_{10}. Labeled components encompass a tangentially cut cell surface complex (SC), a cross-cut "infraciliary lattice" (IL) bundle, a "kinodesmal fiber" (arrowhead) attached to a ciliary basal body (BB), and two parasomal sacs (PS). Bar = 0.1 μm.

Figure 11 Abs against CaN-A detected by pA–Au_5 (arrowheads), mainly at the docking site of a trichocyst (T). Bar = 0.1 μm.

others. In *Paramecium*, there are only indirect hints as to the identity of CaN substrates (see below).

The Abs recognizing the entire CaN molecule (type R299), i.e., subunits A and B, may be useful to recognize CaN on sections, because they have been extensively probed on Western blots (Kissmehl et al. 1997; Hens et al. 1998). From the published sequences retrieved from the EMBL data bank for *Paramecium* and bovine CaN-A, we derive an overall identity of 40% for CaN-A and of 78% for its subunit B-binding domain (data not shown).

Although not yet established for CaN-B of *Paramecium*, association with membranes may be facilitated by myristoylation (Boutin 1997). Occurrence of a binding site for the B-subunit in the A-subunit (Klee et al. 1998) may explain why both subunits show about the same distribution in our cells, although co-localization studies appear to us to be less reliable because of the lower antigenicity of Abs against the B-subunit.

CaN at the Infraciliary Lattice

One of the main components of the dominant cortical filament system in *Paramecium*, the infraciliary lattice, is centrin (Garreau De Loubresse et al. 1991). Although the gene of this 23–24-kD large contractile protein has been cloned in *Paramecium* (Madeddu et al. 1996; Klotz et al. 1997), detailed information on its potential phosphorylation is still required. In the *Paramecium* cortex, Abs against Ser/Thr phosphorylation sites recognize a variety of proteins of ⩾20 kD (Keryer et al. 1987), and cortical morphogenesis depends on the phosphorylation state of some basal body-associated proteins (Sperling et al. 1991), as shown, e.g., in Figure 10. Attached materials may also contain centrin (Levy et al. 1996). CaN can therefore be considered a candidate for regulating centrin-based processes and morphogenesis. In fact, in the flagellate green alga *Tetraselmis*, centrin is dephosphorylated in response to increased cytosolic Ca^{2+} concentrations (Martindale and Salisbury 1990).

CaN at Outlines of Alveolar Sacs and at Trichocyst Docking Sites

Paramecium was the first system for which involvement of CaN in exocytosis regulation could be demonstrated. Microinjection of anti-CaN Abs inhibited trichocyst exocytosis (Momayezi et al. 1987). Since

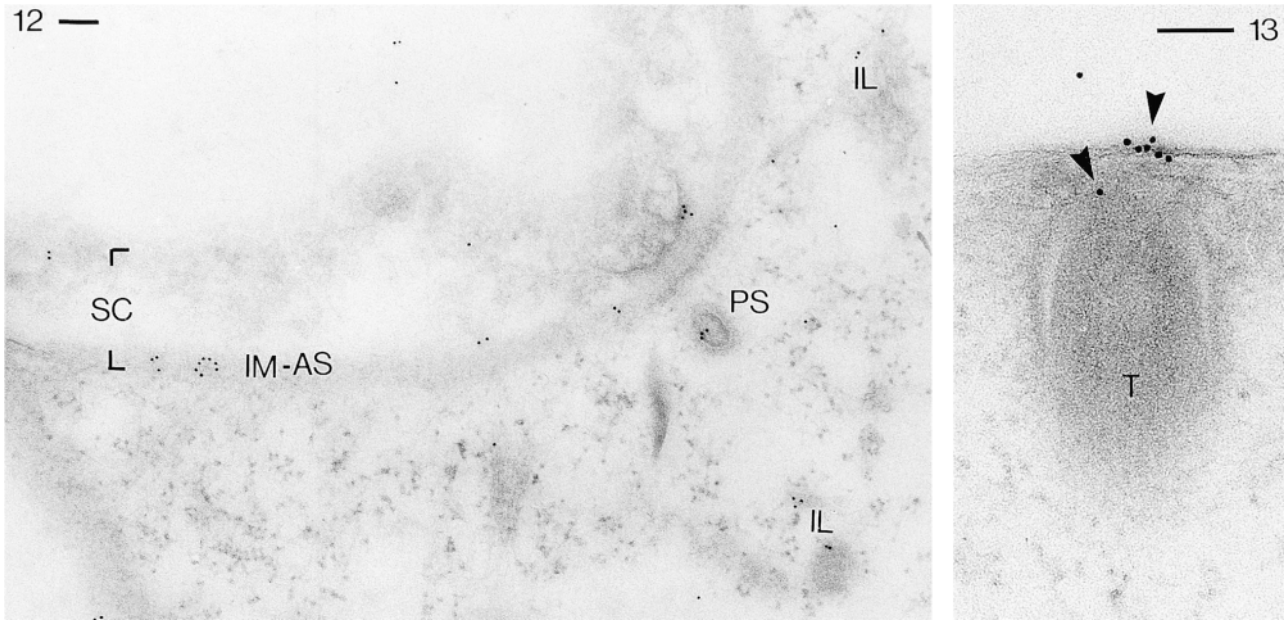

Figure 12 Labeling by Abs against CaN-B followed by GαR–Au_{10}. Gold grains occur on the cell surface complex (SC), particularly along the inner membrane of alveolar sacs (IM-AS) cut at an oblique angle, as well as on a parasomal sac (PS) and portions of "infraciliary lattice" (L) filament bundles. Bar = 0.1 μm.

Figure 13 Abs against CaN-B detected by pA–Au_{10} (arrowheads), mainly at a trichocyst (T) docking site. Bar = 0.1 μm.

then, a stimulatory effect of CaN has been reported for mast cells (Hultsch et al. 1998), T-lymphocytes (Trenn et al. 1989), pancreatic acinar cells (Groblewski et al. 1994), gastric chief cells (Raufman et al. 1997), glutaminergic nerve terminals (Nichols et al. 1994), and for catecholamine- and neuropeptide-releasing cells (Hens et al. 1998). However, inhibitory effects of CaN stimulation have also been occasionally observed, such as for lactotrophic pituitary cells (Fomina and Levitan 1997). This is not surprising, considering the multiple molecular activities that may contribute to such complex activities as exocytosis, e.g., in neurons (Yakel 1997), and the effect may also vary depending on the mode of stimulation. Multiple effects can be envisaged even in a single cell.

In the *Paramecium* cell cortex, distribution of CaN coincides in part with that of the exocytosis-sensitive PP63/parafusin (Kissmehl et al. 1998), because they both are enriched around alveolar sacs and at trichocyst docking sites. With PP63/parafusin, as with calmodulin (Momayezi et al. 1986; Kerboeuf et al. 1993) and CaN (this study), this includes the site of contact between a trichocyst membrane and the cell membrane, the contact site between a trichocyst membrane and alveolar sacs, and the subsequent region called "collar" (dense material surrounding the uppermost portion of a trichocyst). In agreement with this, CaN can dephosphorylate PP63/parafusin (Kissmehl et al. 1996), which in vivo is multiply phosphorylated at Ser and Thr sites (Kussmann et al. 1999) and dephosphorylated strictly in parallel with exocytosis performance (Zieseniss and Plattner 1985). During trichocyst exocytosis, Ca^{2+} concentrations rise to $\sim$5 μM (Klauke and Plattner 1997), i.e., a value appropriate to activate PP2B activity in the cortex of different cells (Yakel 1997). Because in *Paramecium* this involves Ca^{2+} release from alveolar sacs (Länge et al. 1995; Plattner et al. 1997a), it is interesting to note that Ca^{2+} release channels are known to be sensitive to CaN (or CaN-directed drugs) in some other systems (Brillantes et al. 1994; Schuhmann et al. 1997; Wagenknecht and Radermacher 1997; Xiao et al. 1997).

In summary, it remains to be analyzed in more detail whether in *Paramecium* CaN can act precisely at the exocytosis site and/or at the cortical calcium stores.

CaN at Parasomal Sacs

Detachment of clathrin-coated pits from the cell membrane during endocytotic vesicle formation depends on CaN-mediated dephosphorylation of the large monomeric GTP-binding protein dynamin (Liu et al. 1994; Robinson et al. 1994; Marks and McMahon 1998). Although this has been documented thus far mainly with neurons, it may apply to different systems. In *Paramecium* such coated pits, designated

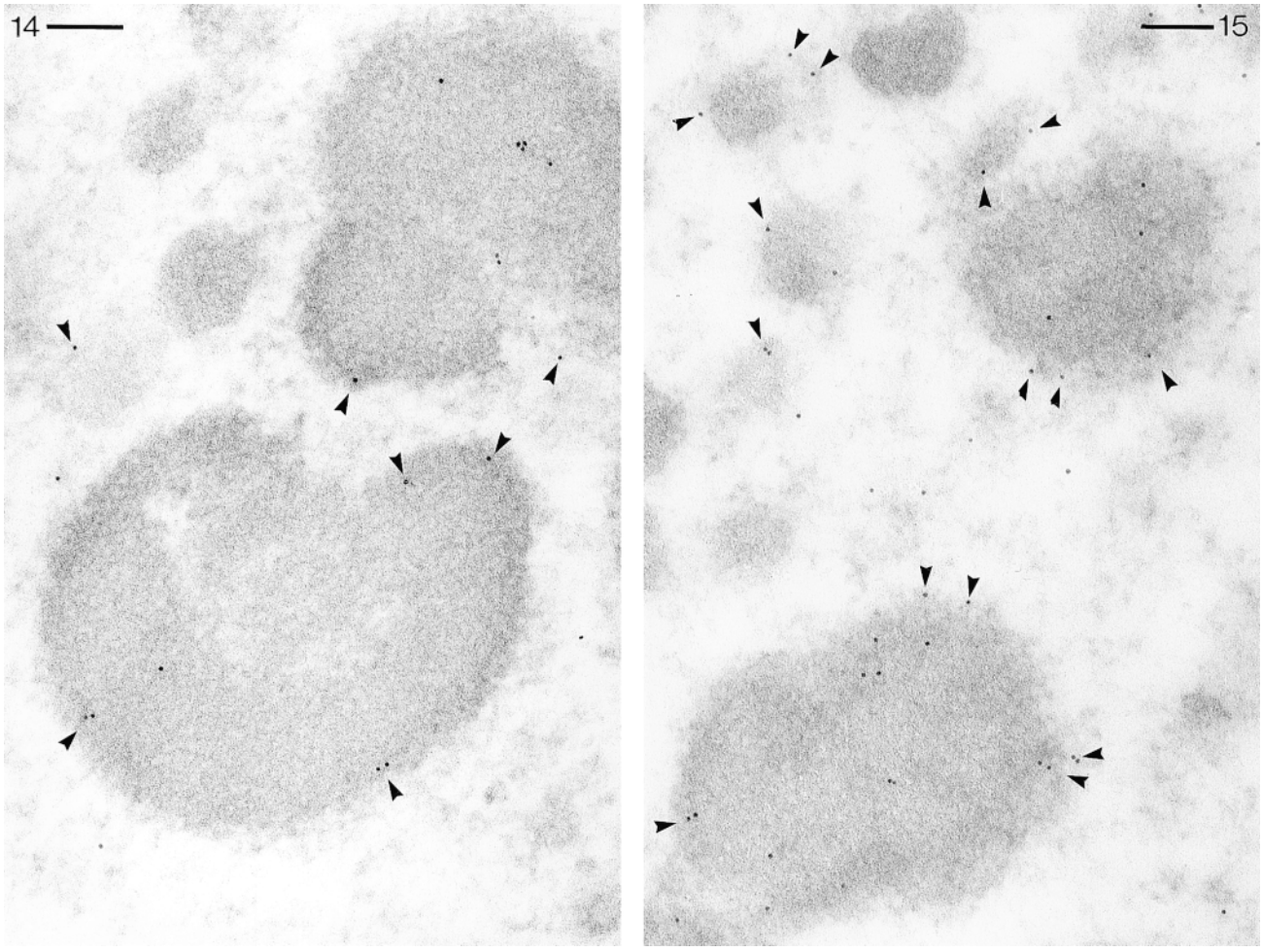

Figure 14 Abs against the CaN-A subunit detected by pA–Au_5 in a macronucleus. Note occurrence of label almost exclusively over heterochromatic areas, frequently along their borders (arrowheads). Bar = 0.1 μm.

Figure 15 Abs against the CaN-B subunit visualized by pA–Au_5 in a macronucleus preferentially labels the rims of heterochromatic zones (arrowheads). Bar = 0.1 μm.

"parasomal sacs," accompany ciliary bases. Regulation of their formation by CaN is suggested by the heavy labeling we observe, although dynamin in our system still remains to be identified at the molecular level.

CaN in the Nucleus

Thus far, CaN has been localized, at the light microscopic level only, in the nuclei of mouse spermatids (Moriya et al. 1995). The involvement of CaN in gene transcription is well established. CaN may facilitate the import of transcription factors (Shibasaki et al. 1996) or may be involved in intranuclear regulation processes. Among them is one of the mechanisms participating in T-lymphocyte activation (Trenn et al. 1989; McKeon 1991; Guerini 1997). Because CaN activates transcription in widely different cell types, such as yeast (Hirata et al. 1995), muscle (Chin et al. 1998), pituitary cells (Lee et al. 1999), and neurons (Yakel 1997), we can now expect similar CaN activities in *Paramecium*.

Acknowledgments

Supported by a grant from the Deutsche Forschungsgemeinschaft, Schwerpunkt "Struktur und Funktionssteuerung an Zelloberflächen."

We are grateful to Dr Karin Hauser for calculating sequence identities, to Sylvia Kolassa for skillful technical assistance, and to Anne Keller for revising the English text.

Literature Cited

Aitken A, Klee CB, Cohen P (1984) The structure of the B subunit of calcineurin. Eur J Biochem 139:663–671

Barford D (1996) Molecular mechanisms of the protein serine/threonine phosphatases. Trends Biochem Sci 21:407–412

Bittermann AG, Knoll G, Németh A, Plattner H (1992) Quantitative immuno-gold labelling and ultrastructural preservation after cryofixation (combined with different freeze-substitution and embedding protocols) and after chemical fixation and cryosectioning. Analysis of the secretory organelle matrix of Paramecium trichocysts. Histochemistry 97:421–429

Boutin JA (1997) Myristoylation. Cell Signal 9:15–35

Brillantes AMB, Ondrias K, Scott A, Kobrinsky E, Ondriasova E, Moschella MC, Jayaraman T, Landers M, Ehrlich BE, Marks AR (1994) Stabilization of calcium release channel (ryanodine receptor) function by FK506-binding protein. Cell 77:513–523

Chin ER, Olson EN, Richardson JA, Yang Q, Humphries C, Shelton JM, Wu H, Zhu W, Bassel–Duby R, Williams RS (1998) A calcineurin-dependent transcriptional pathway controls skeletal muscle fiber type. Genes Dev 12:2499–2509

Cohen PTW (1997) Novel protein serine/threonine phosphatases: variety is the spice of life. Trends Biochem Sci 22:245–251

Cyert MS, Thorner J (1992) Regulatory subunit (CNB1 gene product) of yeast Ca^{2+}/calmodulin-dependent phosphoprotein phosphatases is required for adaptation to pheromone. Mol Cell Biol 12:3460–3469

Dammann H, Hellstern S, Husain Q, Mutzel R (1996) Primary structure, expression and developmental regulation of a Dictyostelium calcineurin A homologue. Eur J Biochem 238:391–399

Desdouits F, Sciliano JC, Greengard P, Girault JA (1995) Dopamine- and cAMP-regulated phosphoprotein DARPP-32: phosphorylation of Ser-137 by casein kinase I inhibits dephosphorylation of Thr-34 by calcineurin. Proc Natl Acad Sci USA 92:2682–2685

Flötenmeyer M, Momayezi M, Plattner H (1999) Immunolabeling analysis of biosynthetic and degradative pathways of cell surface components (glycocalyx) in Paramecium cells. Eur J Cell Biol 78:67–77

Fomina AF, Levitan ES (1997) Control of Ca^{2+} channel current and exocytosis in rat lactotrophs by basally active protein kinase C and calcineurin. Neuroscience 78:523–531

Garreau De Loubresse N, Klotz C, Viguès B, Rutin J, Beisson J (1991). Ca^{2+}-binding proteins and contractility of the infraciliary lattice in Paramecium. Biol Cell 71:217–225

Groblewski GE, Wagner ACC, Williams JA (1994) Cyclosporin A inhibits Ca^{2+}/calmodulin-dependent protein phosphatase and secretion in pancreatic acinar cells. J Biol Chem 269:15111–15117

Groblewski GE, Yoshida M, Bragado MJ, Ernst SA, Leykam J, Williams JA (1998) Purification and characterization of a novel physiological substrate for calcineurin in mammalian cells. J Biol Chem 273:22738–22744

Grothe K, Hanke C, Momayezi M, Kissmehl R, Plattner H, Schultz JE (1998) Functional characterization and localization of protein phosphatase type 2C from Paramecium. J Biol Chem 273: 19167–19172

Guerini D (1997) Calcineurin: not just a simple protein phosphatase. Biochem Biophys Res Commun 235:271–275

Guerini D, Klee CB (1991) Structural diversity of calcineurin, a Ca^{2+} and calmodulin-stimulated protein phosphatase. In Merlevede W, ed. Advances in Protein Phosphatases. Vol 6. Leuven, Belgium, Leuven University Press, 391–410

Hens JJH, DeWit M, Ghijsen WEJ, Leenders AGM, Boddeke HWG, Kissmehl R, Wiegant VM, Weller U, Gispen WH, DeGraan PNE (1998) Role of calcineurin in Ca^{2+}-induced release of catecholamines and neuropeptides. J Neurochem 71:1978–1986

Hinrichsen RD, Fraga D, Russell C (1995) The regulation of calcium in Paramecium. Adv Second Mess Phosphoprot Res 30:311–338

Hirata D, Harada SI, Namba H, Miyakawa T (1995) Adaptation to high-salt stress in Saccharomyces cerevisiae is regulated by Ca^{2+}/calmodulin-dependent phosphoprotein phosphatase (calcineurin) and cAMP-dependent protein kinase. Mol Gen Genet 249:257–267

Huang S, Merat D, Cheung WY (1989) Phosphatidylinositol modulates the response to calmodulin-dependent phosphatase to calmodulin. Arch Biochem Biophys 270:42–49

Hultsch T, Brand P, Lohmann S, Saloga J, Kincaid RL, Knop J (1998) Direct evidence that FK506 inhibition of F_c epsilon RI-mediated exocytosis from RBL mast cells involves calcineurin. Arch Dermatol Res 290:258–263

Inagaki N, Ito M, Nakano T, Inagaki M (1994) Spatiotemporal distribution of protein kinase and phosphatase activities. Trends Biochem Sci 19:448–452

Kerboeuf D, LeBerre A, Dedieu JC, Cohen J (1993) Calmodulin is essential for assembling links necessary for exocytotic membrane fusion in Paramecium. EMBO J 12:3385–3390

Keryer G, Davis FM, Rao PN, Beisson J (1987) Protein phosphorylation and dynamics of cytoskeletal structures associated with basal bodies in Paramecium. Cell Motil Cytoskel 8:44–54

Kissmehl R, Hauser K, Gössringer M, Momayezi M, Klauke N, Plattner H (1998) Immunolocalization of the exocytosis-sensitive phosphoprotein, PP63/parafusin, in Paramecium cells using antibodies against recombinant protein. Histochem Cell Biol 110:1–8

Kissmehl R, Treptau T, Hofer HW, Plattner H (1996) Protein phosphatase and kinase activities possibly involved in exocytosis regulation in Paramecium tetraurelia. Biochem J 317:65–76

Kissmehl R, Treptau T, Kottwitz B, Plattner H (1997) Occurrence of a para-nitrophenyl phosphate-phosphatase with calcineurin-like characteristics in Paramecium tetraurelia. Arch Biochem Biophys 344:260–270

Klauke N, Plattner H (1997) Imaging of Ca^{2+} transients induced in Paramecium cells by a polyamine secretagogue. J Cell Sci 110: 975–983

Klee CB, Ren H, Wang X (1998) Regulation of the calmodulin-stimulated protein phosphatase, calcineurin. J Biol Chem 273: 13367–13370

Klotz C, Garreau De Loubresse N, Ruiz F, Beisson J (1997) Genetic evidence for a role of centrin-associated proteins in the organization and dynamics of the infraciliary lattice in Paramecium. Cell Motil Cytoskel 38:172–186

Kussmann M, Hauser K, Kissmehl R, Breed J, Plattner H, Roepstorff P (1999) Comparison of in vivo and in vitro phosphorylation of the exocytosis-sensitive protein PP63/parafusin by differential MALDI mass spectrometric peptide mapping. Biochemistry 38:7780–7790

Länge S, Klauke N, Plattner H (1995) Subplasmalemmal Ca^{2+} stores of probable relevance for exocytosis in Paramecium. Alveolar sacs share some but not all characteristics with sarcoplasmic reticulum. Cell Calcium 17:335–344

Lee HW, Hahm SH, Hsu CM, Eiden LE (1999) Pituitary adenylate cyclase-activating polypeptide regulation of vasoactive intestinal polypeptide transcription requires Ca^{2+} influx and activation of the serine/threonine phosphatase calcineurin. J Neurochem 73: 1769–1772

Levy YY, Lai EY, Remillard SP, Heintzelman MB, Fulton C (1996) Centrin is a conserved protein that forms diverse associations with centrioles and MTOCs in Naegleria and other organisms. Cell Motil Cytoskel 33:298–323

Liu JP, Sim ATR, Robinson PJ (1994) Calcineurin inhibition of dynamin I GTPase activity coupled to nerve terminal depolarization. Science 265:970–973

Lukyanetz EA (1997) Evidence for colocalization of calcineurin and calcium channels in dorsal root ganglion neurons. Neuroscience 78:625–628

Madeddu L, Klotz C, LeCaer JP, Beisson J (1996) Characterization of centrin genes in Paramecium. Eur J Biochem 238:121–128

Marks B, McMahon HT (1998) Calcium triggers calcineurin-dependent synaptic vesicle recycling in mammalian nerve terminals. Curr Biol 8:740–749

Martindale VE, Salisbury JL (1990) Phosphorylation of algal centrin is rapidly responsive to changes in the external milieu. J Cell Sci 96:395–402

McKeon F (1991) When worlds collide: immunosuppressants meet protein phosphatases. Cell 66:823–826

Momayezi M, Habermann AW, Sokolova JJ, Kissmehl R, Plattner H (1993) Ultrastructural and antigenic preservation of a delicate structure by cryopreparation: identification and immunogold lo-

calization during biogenesis of a secretory component (membrane–matrix connection) in *Paramecium* trichocysts. J Histochem Cytochem 41:1669–1677

Momayezi M, Kersken H, Gras U, Vilmart–Seuwen J, Plattner H (1986) Calmodulin in *Paramecium tetraurelia*: localization from the in vivo to the ultrastructural level. J Histochem Cytochem 34:1621–1638

Momayezi M, Lumpert CJ, Kersken H, Gras U, Plattner H, Krinks MH, Klee CB (1987) Exocytosis induction in Paramecium tetraurelia cells by exogenous phosphoprotein phosphatase in vivo and in vitro. Possible involvement of calcineurin in exocytotic membrane fusion. J Cell Biol 105:181–189

Momayezi M, Wloga D, Kissmehl R, Plattner H, Jung G, Klumpp S, Schultz JE (1996) Immunolocalization of protein phosphatase type 1 in Paramecium cells using antibodies against recombinant protein and peptides. J Histochem Cytochem 44:891–905

Moriya M, Fujinaga K, Yazawa M, Katagiri C (1995) Immunohistochemical localization of the calcium/calmodulin-dependent protein phosphatase, calcineurin, in the mouse testis: its unique accumulation in spermatid nuclei. Cell Tissue Res 281:273–281

Nichols RA, Suplick GR, Brown JM (1994) Calcineurin-mediated protein dephosphorylation in brain nerve terminals regulates the release of glutamate. J Biol Chem 269:23817–23823

Perrino BA, Soderling TR (1998) Biochemistry and pharmacology of calmodulin-regulated phosphatase calcineurin. In Van Eldik LJ, Watterson DM, eds. Calmodulin and Signal Transduction. San Diego, London, Boston, Academic Press, 170–236

Plattner H, Braun C, Hentschel J (1997a) Facilitation of membrane fusion during exocytosis and exocytosis-coupled endocytosis and acceleration of "ghost" detachment in Paramecium by extracellular calcium. A quenched-flow/freeze-fracture analysis. J Membr Biol 158:197–208

Plattner H, Habermann A, Kissmehl R, Klauke N, Majoul I, Söling HD (1997b) Differential distribution of calcium stores in Paramecium cells. Occurrence of a subplasmalemmal store with a calsequestrin-like protein. Eur J Cell Biol 72:297–306

Plattner H, Zingsheim HP (1983) Electron microscopic methods in cellular and molecular biology. Subcell Biochem 9:1–236

Pouphile M, Lefort–Tran M, Plattner H, Rossignol M, Beisson J (1986) Genetic dissection of the morphogenesis of exocytosis sites in Paramecium. Biol Cell 56:151–162

Quinlan EM, Halpain S (1996) Emergence of activity-dependent, bidirectional control of microtubule-associated protein MAP2 phosphorylation during postnatal development. J Neurosci 16: 7627–7637

Raufman JP, Malhotra R, Raffaniello RD (1997) Regulation of calcium-induced exocytosis from gastric chief cells by protein phosphatase-2B (calcineurin). Biochim Biophys Acta 1357:73–80

Reynolds ES (1963) The use of lead citrate at high pH as an electron-opaque stain in electron microscopy. J Cell Biol 17:208–212

Robinson PJ, Liu JP, Powell KA, Fykse EM, Südhof TC (1994) Phosphorylation of dynamin I and synaptic-vesicle recycling. Trends Neurosci 17:348–353

Schuhmann K, Romanin C, Baumgartner W, Groschner K (1997) Intracellular Ca^{2+} inhibits smooth muscle L-type Ca^{2+} channels by activation of protein phosphatase type 2B and by direct interaction with the channel. J Gen Physiol 110:503–513

Shenolikar S (1994) Protein serine/threonine phosphatases—new avenues for cell regulation. Annu Rev Cell Biol 10:55–86

Shibasaki F, Price ER, Milan D, McKeon F (1996) Role of kinases and the phosphatase calcineurin in the nuclear shuttling of transcription factor NF-AT4. Nature 382:370-373

Sperling L, Keryer G, Ruiz F, Beisson J (1991) Cortical morphogenesis in Paramecium: a transcellular wave of protein phosphorylation involved in ciliary rootlet disassembly. Dev Biol 148:205–218

Stelly N, Mauger JP, Keryer G, Claret M, Adoutte A (1991) Cortical alveoli of Paramecium: a vast submembranous calcium storage compartment. J Cell Biol 113:103–112

Sugimoto T, Stewart S, Guan KL (1997) The calcium/calmodulin-dependent protein phosphatase calcineurin is the major Elk-1 phosphatase. J Biol Chem 272:29415–29418

Trenn G, Taffs R, Hohman R, Kincaid R, Shevach EM, Sitkovsky M (1989) Biochemical characterization of the inhibitory effect of CsA on cytolytic T lymphocyte effector functions. J Immunol 142:3796–3802

Turner KM, Burgoyne RD, Morgan A (1999) Protein phosphorylation and the regulation of synaptic membrane traffic. Trends Neurosci 22:459–464

Valdivia HH (1998) Modulation of intracellular Ca^{2+} levels in the heart by sorcin and FKBP12, two accessory proteins of ryanodine receptors. Trends Pharmacol Sci 19:479–482

Venable JH, Coggeshall R (1965) A simplified lead citrate stain for use in electron microscopy. J Cell Biol 25:407–408

Vincent JB, Crowder MW (1995) Phosphoprotein serine/threonine phosphatases. In Vincent JB, Crowder MW, eds. Phosphatases in Cell Metabolism and Signal Transduction: Structure, Function and Mechanism of Action. Heidelberg, New York, Berlin, Springer-Verlag, 7–60

Wagenknecht T, Radermacher M (1997) Ryanodine receptors: structure and macromolecular interactions. Curr Opin Struct Biol 7:258–265

Xiao RP, Valdivia HH, Bogdanov K, Valdivia C, Lakatta EG, Cheng H (1997). The immunophilin FK506-binding protein modulates Ca^{2+} release channel closure in the heart. J Physiol 500:343–354

Yakel JL (1997) Calcineurin regulation of synaptic function: from ion channels to transmitter release and gene transcription. Trends Pharmacol Sci 18:124–134

Zieseniss E, Plattner H (1985) Synchronous exocytosis in Paramecium cells involves very rapid ($\leqslant$1 s), reversible dephosphorylation of a 65 kD phosphoprotein in exocytosis-competent strains. J Cell Biol 101:2028–2035